An Adaptive Metric Model for Collective Motion Structures in Dynamic Environments

Stef Van Havermaet[1][0000−0002−5060−6807], Pieter Simoens[1][0000−0002−9569−9373], and Yara Khaluf[2][0000−0002−5590−9321]

[1] Department of Information Technology–IDLab, Faculty of Engineering and Architecture, Ghent University–imec, Ghent, Belgium
{stef.vanhavermaet,pieter.simoens}@ugent.be
[2] Department of Social Sciences – INF, Applied Information Science, Wageningen University and Research, Wageningen, The Netherlands
yara.khaluf@wur.nl

Abstract. Robot swarms often use collective motion. Most models generate collective motion using the repulsion zone, alignment zone, and attraction zone. Despite being widely used, these models have a limited capacity for generating group structures in response to environmental stimuli. Enabling robot swarms to display proper spatial structures is crucial for several swarm robotics tasks. In this paper, we focus on three spatial structures that allow the swarm to adapt its aggregation (coverage) and alignment (order) in response to environmental changes. We show that the metric and long-range models are unable to generate every structure. We propose an extension to the metric model that allows the swarm to display the three structures, which is demonstrated in a simulated dynamic environment where different stimuli appear over time.

1 Introduction

Collective motion is nature's most fundamental demonstration of coordinated activity, performed by bird flocks, fish shoals, and human crowds [25]. Emergent behavior results from individuals' interactions to perform tasks like foraging or migrating. Collective motion is important in artificial systems like robot swarms, which simulate social animal behavior. Individual robots have basic abilities, but when they work together in groups, they can perform more complex behaviors like foraging [19,7,17,16], exploration [20,10], and collective perception [23,12].

Many activities in robot swarms need collective motion. Navigation from a source to a destination, forming topologies, tracking targets, and moving objects are among the examples. Depending on the particular task, specific structures need to be displayed in the swarm. For example, the swarm needs to aggregate while navigating through narrow paths, and to expand while exploring new environments. A large number of theoretical [4,6] and empirical [3,11] studies have proposed models to generate collective motion. Most of these models consider short-range repulsion and long-range attraction among the individuals, in addition to the alignment of velocities along with the their (nearest) neighbors

[25]. These models show high efficiency in generating aligned motion based on simple individual rules. However, there is little to no evidence on whether such models can modify spatial features of the group (e.g., structure) as a response to environmental stimuli.

In this study, we use two system measures to define our target structures: swarm order (an expression of alignment degree) and swarm relative coverage (an expression of compactness). The swarm displays three target structures based on environmental stimuli: (a) high coverage, low order (HCLO), (ii) high coverage, high order (HCHO), and (iii) low coverage, high order (LCHO). Individuals have different orientations in HCLO to maximize coverage (low order). This structure is desired for exploration tasks, where robots must observe the environment in all directions and maximize inter-individual distance. HCHO is a high-order, high-coverage swarm. This structure navigates tasks while maximizing coverage (e.g., navigation with exploration). In LCHO, the swarm aggregates, maintaining a high order and high density. This structure can transport items or navigate narrow spaces. All three structures require swarm connectivity (i.e., remain in a single cluster). The aforementioned tasks can also be combined (e.g. search and rescue), which requires the swarm to adapt its structure based on observed stimuli in the dynamic environment.

We consider two models of collective motion: the metric model, where each individual interacts within a defined radius, and the long-range model, where short-interactions occur topologically and long-range interactions randomly. Our results highlight the metric model and long-range model's limitations to generate the above-mentioned structures. We propose an extension to the metric model that allows the swarm to switch between the three structures. We test our extended metric model (EMM) in a simulated dynamic environment, where different stimuli appear over time and are perceived by few individuals.

We show how HCLO, HCHO, and LCHO emerged and how EMM scales with system size. This paper continues as follows. In Section 2, we review collective motion models. In Section 3, we describe the other models we use. In Section 4, we discuss the key results. Section 5 concludes this paper.

2 Related Work

To generate collective motion and group cohesion, many models have been proposed. Models from biology and physics [21,9,13,24,8] suggest simple rules of interaction among individuals can induce collective motion. Such rules capture attraction, repulsion, and alignment [21]. Most of these models use metric distance. These models assume individuals align and attract each other, and that interaction declines with distance. Vicsek model [25] uses neighbor's velocity to exploit individuals' alignment. The Couzin model [5] is used in theoretical biology and group robotics. This paper uses the Couzin model.

Special cases of the metric model were suggested and became widely used, such as the topological model [2,1], in which each individual interacts with a fixed number of neighbors.The topological model was suggested based on ex-

perimental findings of birds flocking [1]. The model proposed in [18] accounts for sensory-imposed interaction limitations, and is a special-case of the metric model. Individuals only interact with visually observable neighbors. In [26], the authors show how long-range models, which introduce long-range alignment interactions between individuals, prevents group dispersion in open spaces.

Several studies have examined spatial structures in natural organisms. [14] studied Zebrafish shoals and schools. This work investigated model parameters other than group density that may impact these two structures. Both [5,22] studied how individual heterogeneity affects spatial position in the group, leading to specific structures. In [15], the authors highlight the importance of system size and the number of influential neighbors on the emergence of different structures. Despite interesting results, the work doesn't explain how the model can generate spatial structures. The obtained structures were dispersed rather than clustered.

3 Model

3.1 Metric and Long-Range Model

Each individual i updates its direction of motion based on the neighbors' poses in the three non-overlapping behavioral zones around i. Each behavioral zone corresponds to a distinct interaction; (i) repulsion from others inside the circular zone with radius ZoR, (ii) alignment of orientation with others inside the zone with width ZoO, and (iii) attraction to others inside the zone with width ZoA.

The metric and long-range models differ from each other by neighbor selection. For the metric model, the neighbors $\mathcal{N}_i$ of individual i consists of all individuals within the interaction-radius $RoI = ZoR + ZoO + ZoA$ [5]. For the long-range model, the neighbor set $\mathcal{N}_i$ is the union of the set of m nearest neighbors $\mathcal{M}_i$ and κ_i randomly selected neighbors of $\mathcal{N}_i \setminus \mathcal{M}_i$ [26], where κ_i is sampled from a Poisson distribution with average κ.

Let $\mathcal{N}_i^r$, $\mathcal{N}_i^o$, and $\mathcal{N}_i^a$ denote the distinct subsets of neighbors by separating $\mathcal{N}_i$ based on the repulsion, orientation, and attraction zones respectively. Let us define r_{ij} as the relative position of individual j from i, and q_i as the direction vector. The new direction computed with weights $\alpha_r \geq 0$, $\alpha_o \geq 0$ and $\alpha_a \geq 0$ as:

$$\hat{q}_i(t) = -\alpha_r \sum_{j \in \mathcal{N}_i^r} \frac{r_{ij}(t)}{\|r_{ij}(t)\|} + \alpha_o \sum_{j \in \mathcal{N}_i^o} \frac{q_j(t)}{\|q_j(t)\|} + \alpha_a \sum_{j \in \mathcal{N}_i^a} \frac{r_{ij}(t)}{\|r_{ij}(t)\|} \tag{1}$$

3.2 System Measures

To quantify whether all individuals move in approximately the same direction, we measure the amount of order Ψ defined as $\Psi(t) = \frac{1}{N} \| \sum_{i=1}^{N} q_i(t) \|$. Furthermore, we define the relative coverage as $\Omega(t) = \frac{A(t)}{A(t_0)}$, with A as the area of the convex hull of the set of robots and t_0 as the starting time step. Finally, the number of clusters is measured where individuals i and j are part of the same cluster if their relative distance is lower than the interaction-radius RoI.

3.3 Extended Metric Model (EMM)

Our proposed model, the extended metric model (EMM), relies on adapting the impact of the behavioral orientation zone while following the same neighbor selection approach as the metric model. In order to obtain a relative coverage $\Omega > 1$ with low order $\Psi \approx 0$, we maintain the width of the orientation zone ZoO, but set $\alpha_o = 0$ in Equation (1)—i.e., deactivating the orientation zone. Consequently, individuals are able to spread out until attraction interactions ensure that they remain cohesive. Transitioning to high relative coverage $\Omega > 1$ and high order $\Psi \approx 1$ is then accomplished by resetting $\alpha_o > 0$ (i.e., activating the orientation zone). To obtain a low relative coverage $\Omega < 1$ with high order $\Psi \approx 1$, the width ZoO is decreased while keeping the zone activated ($\alpha_o > 0$).

4 Results and Discussion

We simulate a robot swarm of size N in 2D open space environment. At the beginning of a simulation, robots are placed within a confined box of the size $(\frac{N}{\rho})^{\frac{1}{2}}$ with initial density $\rho = 0.01$. Within this box, both the robots' positions and moving directions are initially uniformly distributed. All simulations are run with $w = \frac{\pi}{2}$, $v = 2$, $\sigma = 0.05$, $\alpha_r = 100$, $\alpha_o = 50$, and $\alpha_a = 1$ based on preliminary simulations to obtain a system of a single cluster. Unless varied, the system size is $N = 100$.

We start with the metric model, looking at the swarm order Ψ, group relative coverage Ω, and the number of clusters (NoC). The emergence of the target structures (i.e., HCLO, HCHO, and LCHO) is investigated using a combination of these system measures. We enable the width of the orientation zone (ZoO) and the attraction zone (ZoA) to vary over the range of $[0 - 100]$ in Figures 1A,B,C, while keeping the width of the repulsion zone constant ($ZoR = 1$). Structures that arise while the swarm is preserved in a single connected cluster (light-gray color in Figure 1), have a low relative coverage and a high group order, which corresponds to the target structure (LCHO). We note that the swarm splitting in numerous clusters fits with the structure of high coverage and low order (HCLO) (left-bottom corner). Finally, the high-coverage, high-order (HCHO) structure is completely absent. The width of the repulsion zone (ZoR) and the orientation zone (ZoO) are then varied throughout a range of $[5 - 30]$ and $[0 - 200]$, respectively, while the width of the attraction zone remains constant ($ZoA = 50$). The LCHO structure is formed when high order corresponds with low relative coverage, as seen in Figures 1D,E,F. However, given a medium level of order with a possibility of more than one cluster, the right-bottom corner shows a likelihood of a high coverage, low order (HCLO) to emerge. Finally, the high-coverage, high-order (HCHO) structure is again absent.

Next, we perform an analysis of the long-range model. The results are shown in Figure 2 for $\kappa = 0.05$ and $\kappa = 0.9$. Our results for $\kappa = 0.05$, in Figures 2A,B,C, show that the swarm can move in a single cluster, while maintaining a low relative coverage, and a high swarm order. This aligns with the structure of low coverage,

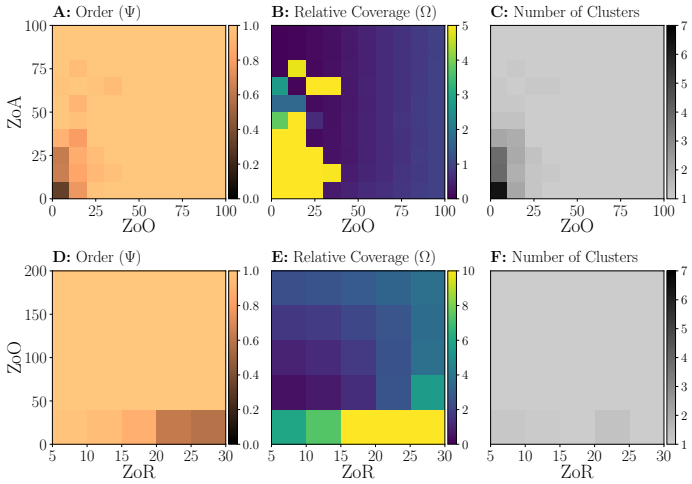

Fig. 1. System measures of the metric model.

high order (LCHO). The other two structures of HCLO and HCHO are fully absent. In Figures 2D,E,F, we can notice an evidence of high relative coverage with high order in the right-bottom corner (while maintaining a single cluster). This corresponds to the structure of HCHO. The long-range model shows similarly to the metric model the ability to generate low coverage, high order structures (LCHO). The structure of high coverage, low order (HCLO) is missing. As the average long-range connectivity κ increases, the long-range model's ability to create a high coverage, high order (HCHO) decreases, as demonstrated in Figure 2G-L. The low coverage, high order (LCHO) structure becomes the only one that the long-range model can generate. Hence, the emergence of the high coverage, high order (HCHO) is κ-dependent for the long-range model.

So far, we have demonstrated that while, both, the metric and the long-range models are suitable to generate the low coverage, high order (LCHO) structures, they are not suitable for generating the other two structures (i.e., HCHO, HCLO). In the following we show the system measures resulting from applying the extended metric model (EMM). Figure 3 demonstrates how the EMM can display the three target structures, while maintaining the group moving in a single cluster for all structures (Figure 3 right column). Figures 3A,B show the system measures when deactivating the orientation zone. Hence the values at the y-axis define the distance at which the attraction zone starts. These two figures show the possibility to generate the HCLO structure through expanding the swarm coverage while pushing the attraction zone away by increasing the width of the deactivated orientation zone. Figures 3D,E are obtained after activating the orientation zone. They show the ability of the EMM model to display, both, the HCHO and the LCHO structures. The HCHO (LCHO) structure is achieved by increasing (decreasing) the width of the activated orientation zone. Both re-

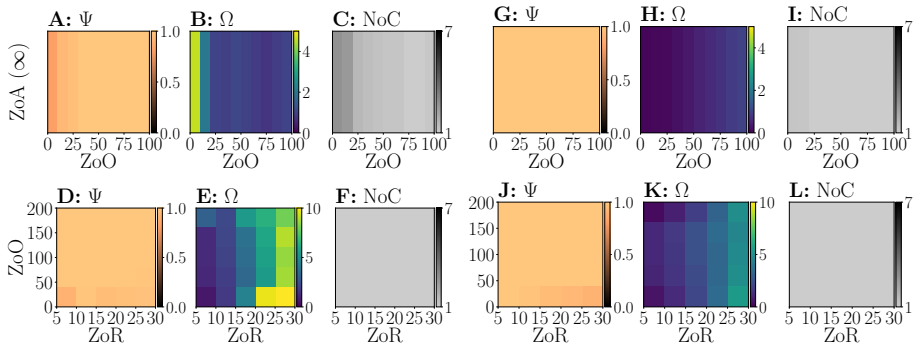

Fig. 2. System measures of the long-range model with $\kappa = 0.05$ (first three columns) and $\kappa = 0.9$ (last three columns).

sults in Figures 3A,B and in Figures 3D,E show that the emerging structure is independent of the width of the repulsion zone (ZoR).

Next, we simulate a swarm of robots using the EMM model to perform the following sequential set of tasks: (i) explore the environment looking for a particular stimulus (**stimulus A**) that define the direction they need to move into. (ii) Navigate in the direction of stimulus A until a **stimulus B** appears. (iii) As a response to stimulus B (e.g., a narrow path) the swarm needs to shrink in coverage while still navigating to its target. Figure 4(left) shows the system measures recorded over 7×10^3 simulated time steps. The swarm order Ψ starts low as the robots are initialized with random directions. Following the EMM model, every robot deactivates its orientation zone, whose width is set to 200, aiming for the HCLO structure. In a few time steps, the relative coverage increases to $\Omega = 3$, while the system maintains a low order. At time step 3×10^3, stimulus A (which triggers the swarm to navigate into one direction) is introduced and perceived by a single robot, who spreads the message to its neighbors. As the message spreads, robots start activating their orientation zone (see Figure 3D,E). This enables the swarm to converge to the HCHO structure after introducing stimulus A, as shown in Figure 4(left). Thanks to activating the orientation zone, fluctuations in both system measures disappear. Finally, at time step 4.5×10^3 stimulus B is introduced and perceived by a single robot, who spread it further. The system converges to the LCHO structure when informed robots reduce the width of their orientation zone. (In this paper, we reduce ZoO to 50 based on findings where we varied ZoO in $[5 - 200]$). Finally, Figure 4(right) shows that the minimum width of the orientation zone, that is needed to create the HCLO and the HCHO structures, scales linearly with the system size.

5 Conclusions

We studied in this paper the emergence of three target structures based on the swarm order and relative coverage; HCLO, HCHO, and LCHO. These structures

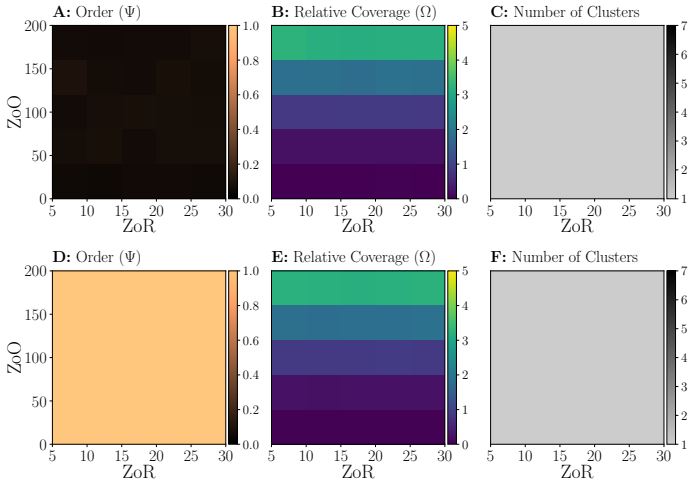

Fig. 3. System measures of the proposed model (EMM).

are fundamental for a large set of robot tasks such as exploration, navigation, and moving through narrow paths. First, we demonstrated that even across a wide range of parameter values, the widely-used metric model and the recently proposed long-range model are unable to generate all three structures. We proposed an extension of the metric model (EMM) that adapts the activation state and width of the orientation zone to dynamically generate the three target structures. We showed that EMM displays each of the three structures in different parameter ranges, and is capable of producing the required structure based on different stimuli introduced in a dynamic environment scenario. We finally show how our model parameter scales linearly with the system size.

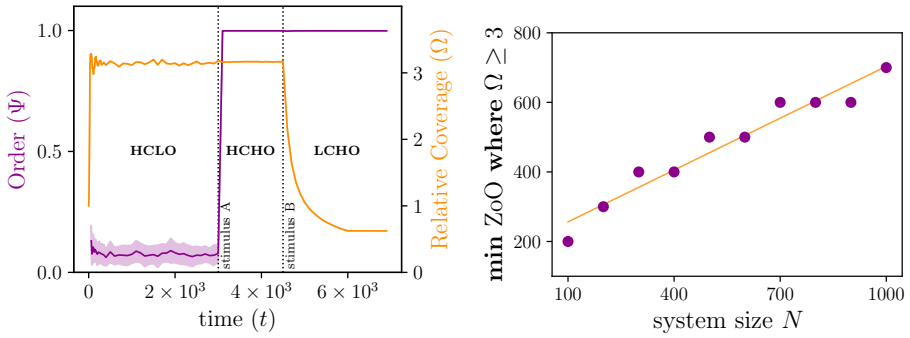

Fig. 4. Further analysis of the proposed model (EMM)

References

1. Ballerini, M., Cabibbo, N., Candelier, R., Cavagna, A., Cisbani, E., Giardina, I., Lecomte, V., Orlandi, A., Parisi, G., Procaccini, A., et al.: Interaction ruling animal collective behavior depends on topological rather than metric distance: Evidence from a field study. Proceedings of the national academy of sciences **105**(4), 1232–1237 (2008)
2. Camperi, M., Cavagna, A., Giardina, I., Parisi, G., Silvestri, E.: Spatially balanced topological interaction grants optimal cohesion in flocking models. Interface focus **2**(6), 715–725 (2012)
3. Cavagna, A., Del Castello, L., Dey, S., Giardina, I., Melillo, S., Parisi, L., Viale, M.: Short-range interactions versus long-range correlations in bird flocks. Physical Review E **92**(1), 012705 (2015)
4. Cavagna, A., Del Castello, L., Giardina, I., Grigera, T., Jelic, A., Melillo, S., Mora, T., Parisi, L., Silvestri, E., Viale, M., et al.: Flocking and turning: a new model for self-organized collective motion. Journal of Statistical Physics **158**(3), 601–627 (2015)
5. Couzin, I.D., Krause, J., James, R., Ruxton, G.D., Franks, N.R.: Collective memory and spatial sorting in animal groups. Journal of theoretical biology **218**(1), 1–11 (2002)
6. Dossetti, V., Sevilla, F.J.: Emergence of collective motion in a model of interacting brownian particles. Physical review letters **115**(5), 058301 (2015)
7. Font Llenas, A., Talamali, M.S., Xu, X., Marshall, J.A., Reina, A.: Quality-sensitive foraging by a robot swarm through virtual pheromone trails. In: International conference on swarm intelligence. pp. 135–149. Springer (2018)
8. Grégoire, G., Chaté, H.: Onset of collective and cohesive motion. Physical review letters **92**(2), 025702 (2004)
9. Huth, A., Wissel, C.: The simulation of the movement of fish schools. Journal of theoretical biology **156**(3), 365–385 (1992)
10. Kegeleirs, M., Garzón Ramos, D., Birattari, M.: Random walk exploration for swarm mapping. In: Annual conference towards autonomous robotic systems. pp. 211–222. Springer (2019)
11. Kelley, D.H., Ouellette, N.T.: Emergent dynamics of laboratory insect swarms. Scientific reports **3**(1), 1–7 (2013)
12. Khaluf, Y., Allwright, M., Rausch, I., Simoens, P., Dorigo, M.: Construction task allocation through the collective perception of a dynamic environment. In: International Conference on Swarm Intelligence. pp. 82–95. Springer (2020)
13. Kunz, H., Hemelrijk, C.K.: Artificial fish schools: collective effects of school size, body size, and body form. Artificial life **9**(3), 237–253 (2003)
14. Miller, N., Gerlai, R.: From schooling to shoaling: patterns of collective motion in zebrafish (danio rerio). PloS one **7**(11), e48865 (2012)
15. Mirabet, V., Auger, P., Lett, C.: Spatial structures in simulations of animal grouping. Ecological modelling **201**(3-4), 468–476 (2007)
16. Nauta, J., Simoens, P., Khaluf, Y.: Group size and resource fractality drive multimodal search strategies: A quantitative analysis on group foraging. Physica A: Statistical Mechanics and its Applications **590**, 126702 (2022)
17. Nauta, J., Van Havermaet, S., Simoens, P., Khaluf, Y.: Enhanced foraging in robot swarms using collective lévy walks. In: 24th European Conference on Artificial Intelligence (ECAI). vol. 325, pp. 171–178. IOS (2020)

18. Poel, W., Winklmayr, C., Romanczuk, P.: Spatial structure and information transfer in visual networks. Frontiers in Physics p. 623 (2021)
19. Rausch, I., Khaluf, Y., Simoens, P.: Scale-free features in collective robot foraging. Applied Sciences **9**(13), 2667 (2019)
20. Rausch, I., Simoens, P., Khaluf, Y.: Adaptive foraging in dynamic environments using scale-free interaction networks. Frontiers in Robotics and AI **7**, 86 (2020)
21. Reynolds, C.W.: Flocks, herds and schools: A distributed behavioral model. In: Proceedings of the 14th annual conference on Computer graphics and interactive techniques. pp. 25–34 (1987)
22. Romey, W.L.: Individual differences make a difference in the trajectories of simulated schools of fish. Ecological Modelling **92**(1), 65–77 (1996)
23. Valentini, G., Brambilla, D., Hamann, H., Dorigo, M.: Collective perception of environmental features in a robot swarm. In: International Conference on Swarm Intelligence. pp. 65–76. Springer (2016)
24. Vicsek, T., Czirók, A., Ben-Jacob, E., Cohen, I., Shochet, O.: Novel type of phase transition in a system of self-driven particles. Physical review letters **75**(6), 1226 (1995)
25. Vicsek, T., Zafeiris, A.: Collective motion. Physics reports **517**(3-4), 71–140 (2012)
26. Zumaya, M., Larralde, H., Aldana, M.: Delay in the dispersal of flocks moving in unbounded space using long-range interactions. Scientific reports **8**(1), 1–9 (2018)